Published in final edited form as:

J Mater Chem B Mater Biol Med. 2015 October 28; 3(40): 7903–7911. doi:10.1039/C5TB00952A.

Hydrogel-Based Engineering of Beige Adipose Tissue

M. K. Vaicik[a,b], **M. Morse**[c], **A. Blagajcevic**[c], **J. Rios**[a], **J. Larson**[a], **F. Yang**[a], **R. N. Cohen**[c], **G. Papavasiliou**[a], and **E. M. Brey**[a,b]

[a]Department of Biomedical Engineering, Illinois Institute of Technology, Chicago, IL

[b]Research Service, Veteran Affairs Hospital, Hines, IL

[c]Section of Endocrinology, Department of Medicine, University of Chicago, Chicago, IL

Abstract

Brown and beige adipose tissues have a significant capacity for energy expenditure that may be exploited as a treatment for obesity and metabolic disease. However, the limited volumes of these tissues in adults hinders realization of this potential. Engineering beige adipose tissue may provide an alternative source of this tissue. In this paper we describe the preparation of poly(ethylene glycol) (PEGDA) hydrogels with mechanical properties similar to native adipose tissue. Adipose derived stem cells (ASC) were cultured in hydrogels without adhesive sequences or degradable monomers. Cells were able to differentiate, independent of scaffold properties and were maintained as a viable and functioning adipose tissue mass. The cells expressed their own basement membrane proteins consistent with the composition of adipose tissue. The ASCs could be induced to express uncoupling protein-1 (UCP-1) and cIDEA, makers of beige adipocytes with expression level varying with hydrogel stiffness. This hydrogel-based culture system serves as a first step in engineering beige adipose tissue.

Graphical Abstract

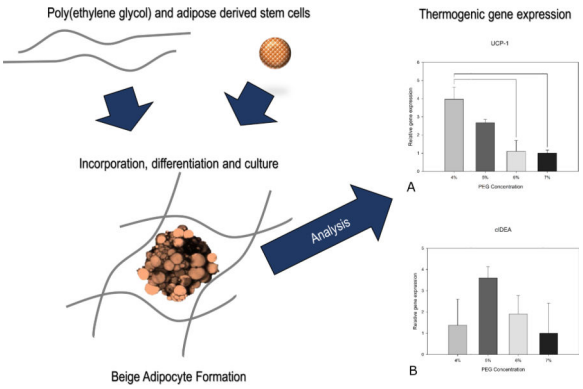

Introduction

The incidence of obesity is increasing globally, generating a burden greater than $190 billion annually on the American healthcare system alone[1]. These costs result primarily from morbidity and mortality associated with the increased incidence of type 2 diabetes, hypertension, heart disease, and certain malignancies in obese and overweight individuals.

Complications from obesity result not only from weight gain directly, but more importantly, from negative metabolic consequences associated with obesity. Adipose is a key endocrine tissue that regulates systemic metabolic function. Studies in pre-clinical models have shown that improvements in the metabolic function of adipose tissue enhances overall metabolic performance[2-4].

There are two main types of adipose tissue, white adipose tissue and brown adipose tissue. White adipose (including subcutaneous white adipose and visceral white adipose) makes up nearly all adipose tissue in adults, with brown adipose present in only small regions of supraclavicular, mediastinal and peri-adrenal depots[5,6]. White adipose is involved in energy storage, structural support and hormone regulation. A number of researchers have investigated biomaterial-based approaches for engineering white adipose, based on the clinical need for new adipose sources for breast reconstruction, soft tissue augmentation and composite tissue reconstruction[7-19]. However, engineering metabolically active brown or beige adipose tissue has not previously been pursued.

Brown adipose tissue has a high capacity for energy expenditure and thermogenesis, and thus has been considered a potential target for the treatment of obesity and metabolic disease[20-23]. Increasing the presence of brown adipose tissue in an individual would be expected to improve overall metabolic function[24, 25], but the small volume of brown adipose in adults suggests that its therapeutic potential may be limited when targeted directly. Alternatively, white adipose tissue can be induced to behave in a manner similar to brown adipose tissue. There is currently incredible enthusiasm for therapeutic induction of this so-called “beige” adipose tissue to increase adipose thermogenic capacity as a treatment for metabolic disease[22, 26-31]. An alternative approach could be to use tissue engineering to generate beige adipose tissue from autologous adipose derived stromal cells (ASCs) that can be transplanted into a patient.

Poly (ethylene glycol) diacrylate (PEGDA) hydrogels have been investigated extensively as scaffolds for tissue engineering. PEGDA hydrogels are resistant to non-specific protein adsorption and cell adhesion, providing an inert starting point for biomaterial design. The hydrogels can be engineered with mechanical properties similar to soft tissues, and fairly straightforward chemistry can be used to incorporate biological signals into the network structure. PEGDA hydrogels are typically prepared such that they are not susceptible to degradation under ambient and/or physiologic conditions.[32] Segments susceptible to hydrolysis or enzymatic cleavage can be readily introduced within network crosslinks allowing for controlled hydrogel degradation. Previous studies have utilized PEG-based hydrogels functionalized with extracellular matrix (ECM)-based attachment sites and enzymatically degradable sequences for 3D adipocyte differentiation[12, 33]. Mesenchymal stem cells encapsulated in PEG hydrogels can be differentiated into adipocytes[34], and thin films of PEG have been utilized to investigate the role of sub-micron topography on preadipocyte behavior[35]. However, PEG hydrogels have not been used as an environment for engineering beige adipose tissue.

In this study, we investigated beige adipocyte formation from ASCs in 3D culture. PEGDA hydrogels were used as a cell culture platform to provide a controlled 3D environment for

cell growth and to investigate the role of matrix stiffness on ASC function. The fundamental design goal for the hydrogels was to mimic the stiffness of adipose tissue. This would allow for investigation of the role of mechanical properties on ASC differentiation into beige adipocytes. The hydrogels were prepared without adhesion sequences or degradable crosslinks. This decouples the mechanical effects from the effects of cell adhesion or degradability of the hydrogel. The hydrogels engineered in a range of mechanical properties approximating those found in adipose tissue by varying the crosslinker content, and the viability and differentiation of ASCs was evaluated. The expression of beige adipose makers, adipogenic markers and extracellular matrix proteins were measured as a function of hydrogel elastic modulus. To our knowledge, this is the first study to apply concepts from tissue engineering to the generation of ***brown or beige adipose tissue***.

Materials and Methods

Chemicals

DMEM/F12, penicillin/streptomycin, and BODIPY 493/503 (4,4-Difluoro-1,3,5,7,8-Pentamethyl-4-Bora-3a,4a-Diaza-s-Indacene) were purchased from Fisher Scientific. Collagenase type I, FBS, HEPES sodium salt, NaCl, HCl, NaOH, eosin Y, N-vinylpyrrolidone (NVP), triethanolamine (TEA), carboxymethylcellulose, indomethacin, dexamethasone (DEX), 3-Isobutyl-1-methylxanthine (IBMX), rosiglitazone, 3,3',5-Triiodo-L-thyronine (T3), and insulin were purchased from Sigma. PEG-diacrylate (PEGDA) macromers were synthesized according to previously published method[36]. The PEGDA purity and structure were verified by ^{1}H NMR (Advance 300 Hz; Bruker). The product was dissolved in CDCl3 with 0.05% tetramethylsilane as an internal standard, to perform ^{1}H NMR.

Cell Isolation and Culture

Subcutaneous adipose depots were harvested from euthanized C57BL/6 male 12-15 week old mice and digested in 500 units activity/ml collagenase type I. All animal procedures were approved by the Institutional Animal Care and Use Committee at the University of Chicago. The adipose derived stem cells (ASC) were enzymatically isolated following a published protocol[37]. Briefly, digestion was performed in an orbital shaker at 37 °C for 60 minutes. The digest was then centrifuged with the floating adipocytes layer discarded. The pelleted stromal vascular fraction was washed twice with media and plated in tissue culture flask. The media used was DMEM/F12 with 10% FBS and 1% penicillin/streptomycin. Cells were incubated at 37 °C and 5% CO_2. Media was changed every 2-3 days.

Spheroid Formation

Cells were trypsinized, counted, and resuspended in DMEM/F12 supplemented with 10% FBS, 1% penicillin/streptomycin, and 0.24% (w/v) carboxymethylcellulose (Sigma) at a density of 20,000 cells/150ul. The solution was pipetted into a non-adherent 96-well U-bottom plate (150 μL/well) (Sigma) and cultured at 37°C and 5% CO_2. Cell spheroids were formed after 24 hours.

PEGDA Hydrogel Formation and Spheroid Encapsulation

Hydrogel precursor solutions were prepared with 8kDa PEGDA at concentrations of 3, 4, 5, 6, and 7% (w/v) in 10 mM HEPES (500 mL ddH_2O, 4 g NaCl, and 1.302 mg HEPES sodium salt; pH balanced to 7.4 with HCl or NaOH) with 0.05 mM eosin Y as the initiator, 225 mM triethanolamine (TEA) as a co-initiator and 37 mM N-vinylpyrrolidone (NVP). Precursor solutions (100 μL/hydrogel) were photopolymerized in the presence of cell spheroids by exposure to visible light (λ = 514 nm) for 15 seconds using an Argon Ion Laser (Coherent, Inc., Santa Clara, CA) at a laser flux of 100 mW/cm^2 (Figure 1). The hydrogels with cell spheroids were removed from the wells, transferred to a 24-well plate and washed 3 times with HEPES buffer solution, immersed in media and incubated at 37 °C and 5% CO_2.

Cell Culture and Differentiation

The hydrogels were cultured for 24 hours in DMEM/F12 with 10% FBS and 1% penicillin/streptomycin. Induction media consisted of DMEM/F12 with 10% FBS, 1% penicillin/streptomycin, 125 μM Indomethacin, 2 μg/mL DEX, 0.5 mM IBMX, 1 nM 3,3',5-Triiodo-L-thyronine (T3), and 5 μg/mL insulin[38]. Induction media was given to the spheroids for 48 hours to induce adipocyte differentiation. Thiazolidinedione (TZD, 0.5 μM rosiglitazone) was added to the media to promote differentiation into beige adipocytes. After 2 days of induction, cells were given maintenance media consisting of DMEM/F12 with 10% FBS, 1% penicillin/streptomycin, 1 nM T3 and 5 μg/mL insulin. Based on published protocols on beige adipocyte stimulation[25, 38, 39], the first two media changes after induction included rosiglitazone. On the first change (day 3), the spheroids were given 0.5 μM rosiglitazone in the maintenance media. On the second change (day 5), the spheroids were supplemented with 1.0 μM rosiglitazone. Maintenance media changes past day 7 did not include rosiglitazone. The hydrogels were cultured for a total of 20 days.

Staining

A LIVE/DEAD® assay kit (Molecular Probes, Inc. Eugene, OR) was used to evaluate cell viability at day 20. Briefly, hydrogels were rinsed with PBS and incubated with LIVE/DEAD staining reagents calcein AM (green fluorescent dye stains live cells) and ethidium homodimer-1 (red fluorescent dye stains dead cells) for 1 h following the manufacturer's protocol. Samples were imaged using confocal laser scanning microscopy Axiovert 200 5x objective (Carl Zeiss MicroImaging, Inc., Thornwood, NY). The percentage of viable cells was quantified by estimating the area of cells in the spheroid stained green ($area_{live}$) and those stained red ($area_{dead}$) using confocal microscopy:

$$\% \quad \text{viable} = \frac{\text{area}_{\text{live}}}{(\text{area}_{\text{live}} + \text{area}_{\text{dead}})}$$

Lipid loading was evaluated with BODIPY staining. Hydrogels containing adipocyte spheroids were incubated in 4% paraformaldehyde overnight. After paraformaldehyde was removed hydrogels were washed two times for thirty minutes each in phosphate buffered saline (PBS). The hydrogels were stained with BODIPY 493/503 (4,4-Difluoro-1,3,5,7,8-

Pentamethyl-4-Bora-3a,4a-Diaza-s-Indacene) at 0.01 mg/ml in PBS at 37°C for 1 hour. Hydrogels were washed two times with PBS and imaged using an Axiovert 200 inverted confocal microscope 10x objective (Carl Zeiss MicroImaging, Inc., Thornwood, NY) at excitation wavelength 488 nm and long pass filter 505 nm.

Swelling Ratio and Mesh Size

Hydrogel swelling was calculated by measuring the ratio of the mass of the swollen gel (M_S) 24 h postphotopolymerization to the mass of the dried gel (M_D). The mass of the swollen hydrogel was measured by removing excess fluid from the hydrogel surface. The mass of the dried hydrogel was measured after drying the hydrogels under vacuum for 24 hours at 50°C. The hydrogel mass swelling ratio (Q_m) was calculated as:

$$Q_m = \frac{M_S}{M_D}$$

Where M_S is the mass of the swollen gel and M_D is the mass of the dried gel. The mesh size (ξ) of the swollen hydrogel was quantified based on the theory of rubber elasticity as previously described[40]:

$$\xi = V_{2,S}^{-\frac{1}{3}} \left(r_o^2\right)^{\frac{1}{2}}$$

In the above $V_{2,S}$ represents the polymer volume fraction of the hydrogel in the swollen state which is also equal to the reciprocal of the volumetric swelling ratio (Q):

$$V_{2,S} = \frac{V_P}{V_S} = \frac{1}{Q}$$

in which V_P refers to the hydrogel volume in the dried state and V_S refers to the hydrogel volume in swollen state. The root mean square unperturbed end to end distance of the polymer chain between crosslinks, $\left(r_o^2\right)^{\frac{1}{2}}$ is given by the following equation:

$$\left(r_o^2\right)^{\frac{1}{2}} = l C_n^{\frac{1}{2}} \left(\frac{2\overline{M_c}}{M_r}\right)^{\frac{1}{2}}$$

The average bond length between the C-C and C-O bonds in the PEG repeat unit is l (l = 1.46 Å), the characteristic ratio of PEG is C_n (C_n = 4) and the molecular weight of the PEG repeat unit is M_r (M_r = 44 g/mol). The average molecular weight between cross-links is $\overline{M_c}$, this value was calculated according to the following equation[41]:

$$\frac{1}{\overline{M_C}}=\frac{2}{\overline{M_n}}-\frac{\left(\frac{v}{V_1}\right)\left[ln\left(1-V_{2,S}\right)+V_{2,S}+\chi_1 {V_{2,S}}^2\right]}{V_{2,r}\left[\left(\frac{V_{2,S}}{V_{2,r}}\right)^{\frac{1}{3}}-\left(\frac{V_{2,S}}{2V_{2,r}}\right)\right]}$$

in which *v* is the specific volume of the polymer (0.84 cm^3/g), V_1 is the molar volume of the solvent (18 cm^3/mol) and $V_{2,r}$ is the polymer volume fraction in the relaxed state immediately after polymerization.

Evaluation of Hydrogel Network Structure on Solute Diffusivity

A theoretical model developed by Lustig and Peppas based on free-volume theory was used to describe the relationship between solute diffusivity and network structure The influence of the hydrogel on solute diffusion was estimated as[42]:

$$\frac{D_g}{D_o}=\left(1-\frac{r_s}{\xi}\right)exp\left(-Y\left(\frac{V_2}{1-V_2}\right)\right)$$

Where D_g is the diffusion coefficient of the solute in the hydrogel, ξ is the mesh size, and V_2 is the polymer volume fraction in the swollen state. Y is the ratio of the required critical volume for successful translational movement of the encapsulated solute and the average free volume per solvent molecule. A reasonable approximation for Y is unity. The diffusion coefficient of the solute in the pure solvent, D_o, can be estimated using the Stokes-Einstein equation:

$$D_o=\frac{kT}{6\pi\eta R_s}$$

where k is Boltzmann's constant (1.38 × 10-23 m^2kg/s^2K); T is temperature (T = 37 °C = 310 K); η is the viscosity of the solvent (6.92 × 10^{-4} kg/ms for water at 37 °C) and R_s is the Stokes radius of the solute [42]. Insulin is a solute in the media that is critical for the cell spheroids within the hydrogel network to receive. Insulin has a hydrodynamic radius of 1.47 nm.

Quantitative Real-time PCR

The hydrogels were flash frozen in liquid nitrogen on days 1 and 20, minced using a razor blade, and processed using Qiagen RNeasy Mini kit for extraction following the manufacturer instructions. The purity and concentration of the isolated RNA was assessed using a Nanodrop 2000. The cDNA was synthesized with Quanta Biosciences Qscript. Quantitative real-time polymerase chain reaction (qRT-PCR) was performed using SYBR green on a Bio-Rad MyiQ RT-PCR detection system (Bio-Rad, Hercules, California). Primers (Table 1) from Integrated DNA Technologies (Coralville, Iowa) were selected from literature or designed using Mouse Primer Depot (http://mouseprimerdepot.nci.nih.gov/) and Primer-Blast (http://www.ncbi.nlm.nih.gov/tools/primer-blast/). Melt curve analysis was used to assess primer specificity.18s rRNA was used as the reference gene to control for

total mRNA recovery. Gene expression levels were evaluated by the ΔΔ threshold cycle (Ct) method[43].

Statistics

The significant differences between the groups of data were determined using analysis of variance (ANOVA) followed with Tukey post test. In all cases, $p<0.05$ was considered significant.

Results

Physical and Mechanical Characterization of PEGDA Hydrogels

PEGDA hydrogels were synthesized using free-radical photopolymerization in the presence of visible light. Hydrogel mechanical properties were varied by altering the PEGDA macromer crosslinker concentration (3%-7% w/vol). The compressive modulus of the PEG hydrogels was found to increase with increasing crosslinker content (Figure 2). The elastic modulus values achieved are within the published range of moduli previously reported for adipose tissue (2-32 kPa) [44, 45]. Increasing the concentration of PEGDA from 4% to 7% also resulted in a statistically significant decrease in both the swelling ratio and mesh size (Figure 3) of the hydrogel network. The 4% and 5% PEGDA hydrogels had a less rigid disc morphology macroscopically compared to the higher compressive modulus hydrogels (6% and 7%) that retained a more defined disc shape after swelling. The ASC cell spheroids on day 1 (Figure 4A-D) the cells appear smooth and elongated within the spheroid after differentiating the cells within the spheroid have rounded and lipid loaded at day 20 (Figure 4E-H and Figure 5A-D). The hydrogel swelling ratio ranged from 41.19 ± 3.83 (4%) to 30.17 ± 9.17 (7%) and the mesh size (ξ) ranged between 10.75 ± 0.399 (4%) and 9.05 ± 0.933nm (7%).

The influence of the network structure on diffusion within the hydrogels was also estimated from theoretical models of free-volume theory. The diffusion coefficient (D_o) of insulin, an important mediator of adipocyte function, in media is 2.23×10^{-6} cm^2/s. Based on the polymer volume fraction and mesh size the diffusion coefficient for insulin within the PEGDA hydrogel (D_g) would range from 1.88×10^{-6} cm^2/s in the 4% PEGDA ($D_g/D_o=0.84$) to 1.81×10^{-6} cm^2/s ($D_g/D_o=0.81$) in the 7% PEGDA hydrogel. These results suggest there is little difference in diffusive resistance between the hydrogel conditions. TZDs have been shown to be helpful for promoting beige adipocyte formation. TZD, rosiglitazone, ($C_{18}H_{19}N_3O_3S$, ~357 Da molecular weight) is much smaller in size than insulin ($C_{256}H_{381}N_{65}O_{76}S_6$, ~5800 Da molecular weight). Less diffusive resistance would be expected for the smaller rosiglitazone in the hydrogels.

Maintenance of a Differentiated Cells in 3D Culture

The spheroids in the hydrogels had a smooth and relatively consistent structure at day 1 independent of crosslinker concentration (Figure 4A-D). After differentiation the spheroid surfaces were rougher with evidence of lipid loading in the cells (Figure 4E-H). The viability of cell spheroids encapsulated in the hydrogels was high (98-99%) under all PEGDA concentrations out to the final time point used in this study (20 days, Figure 5A-

D)). Lipid loading was observed throughout the spheroid volume at all crosslinker concentrations (Figure 5E-H). Both unilocular and multilocular adipocytes were observed within the spheroids in the hydrogels. The cell spheroids did not exhibit expression of the adipocyte marker adiponectin on day 1. However, after 20 days of culture in differentiation media, all groups express adiponectin and peroxidase proliferator-activated receptor gamma (PPARG), markers of adipocyte differentiation, without significant differences in expression level with hydrogels stiffness (Figure 6). Pref-1 a marker of preadipocytes was not expressed at day 20. The cells exhibited high viability and differentiation rates despite using PEGDA hydrogels that did not contain degradable linkages or cell adhesion motifs. PEGDA hydrogels were able to maintain viable, differentiated adipocytes in absence of any exogenous extracellular matrix proteins or peptides, over a range of mechanical properties and physical network structure.

Beige Markers

Mitochondrial uncoupling protein 1 (UCP-1) is utilized in the thermogenesis process in brown and beige adipocytes to uncouple respiration and generate heat. UCP-1 mRNA expression is found in brown and beige adipocytes but is not typically expressed at significant levels in white adipocytes. Cell death-inducing DNA fragmentation factor-alpha-like effector A (cIDEA) is a gene that plays a role in adipocyte thermogenesis and is expressed in beige and brown adipocytes. Under differentiation conditions without the TZD rosiglitazone, the cells did not express markers of beige adipocytes (data not shown). When exposed to rosiglitazone as well as the standard differentiation cocktail, mRNA for the beige markers, UCP-1 and cIDEA, were both upregulated (Figure 7). This agrees with previous studies that show that TZD administration is needed to optimize the development of beige adipocytes[46, 47]. Neither PGC1α nor the brown transcription factor PRDM16 were expressed by the adipocytes treated with TZD.

Interestingly, UCP-1 expression (Figure 7A) showed an inverse relationship with PEGDA concentration. UCP-1 expression decreased with increasing hydrogel stiffness. cIDEA levels (Figure 7B) shared a similar trend of expression decreasing with increasing hydrogel stiffness, however the differences were not significant. Mechanical stiffness has not previously been investigated as playing a role in beige adipocyte formation.

Basement Membrane Proteins

Adipocytes in native tissue are surrounded by a thin extracellular matrix (ECM) structure known as the basement membrane. Collagen IV, laminin α4, laminin α2, and fibronectin-1 are all components of adipose tissue basement membrane. The adipocytes in 3D culture expressed the basement membrane proteins collagen IV, laminin α4, and fibronectin-1 (Figure 8). Laminin α2 was not expressed. The level of the basement membrane components did not vary with hydrogel composition.

Discussion

Biomaterials have been investigated for engineering many different tissues and organs. However, to our knowledge, there have not been previous studies using biomaterials to

generate brown or beige adipose tissue. There is significant interest in the ability to generate beige adipose as a potential treatment for metabolic disease and obesity[22, 26-31]. The transplantation of adipose tissue with “good” metabolic function has been shown to benefit overall metabolic parameters[48, 49] We propose that appropriately engineered beige adipose tissue could be transplanted into diseased patients to improve overall metabolic function.

The starting point for this research was to generate a hydrogel environment that mimics native adipose tissue. PEGDA hydrogels were synthesized with compressive moduli within the range of values previously published for adipose tissue[44, 45]. There are many options for incorporating biological signals into PEGDA hydrogels. However, adipocytes are surrounded by a complex basement membrane that is difficult to recreate in synthetic systems, and the composition of this basement membrane is important in regulating adipose tissue function[50]. The ASCs were cultured in the gels as a spheroid enabling them to produce their own matrix. The adipocytes expressed genes for collagen IV, laminin α4, and fibronectin-1 proteins known to be present in adipose basement membrane. Previous studies have shown that many cells exhibit poor viability in PEG in the absence of ECM-based peptides or proteins[42, 51-53]. However, the cell-to-cell contact and production of their own basement membrane in our system likely allows long term viability and function in the hydrogels.

Under standard adipogenic culture conditions the ASCs differentiated into adipocytes but did not express any markers indicating a beige adipocyte phenotype. However, the addition of the TZD rosiglitazone to the media resulted in both UCP-1 and cIDEA expression. PRDM16, a brown and beige adipocyte marker, was not expressed at significant levels in this study. PRDM16 has been shown to be expressed by beige adipocytes differentiated from subcutanous depot stromal vascular fraction cells cultured in 2D for short term culture (4-8 days) while continuously supplied TZD[25, 29, 39]. However, previous work has shown PRDM16 expression decreased when subcutaneous depot preadipcytes are dosed with TZD for 4 days and then not supplied with TZD for 4 additional *in vitro* culture days[39]. The mitochondrogenesis-promoting gene PGC1α was also not expressed at day 20 in TZD-treated cells either. Other primary cell studies have shown that PGC1α is expressed by adipocytes differentiated from epididymal depot preadipocytes cultured in 2D for short term culture (4-8 days) while continuously supplied TZD[29, 39, 46]. Possibly, PRDM16 and PGC1α expression was not observed due to the transient nature of the TZD exposure. In this study, TZD was supplemented in the culture media for the initial 7 day culture period; for the following 13 days the cells did not receive any TZD.

Interestingly, UCP-1 expression varied with PEGDA stiffness. cIDEA also showed a trend of decreasing levels with PEGDA stiffness. These data suggest that the mechanical properties of the substrate environment influence expression of beige markers. It is not clear why beige markers would vary with hydrogel stiffness. To our knowledge there are no data on the influence of mechanical properties on beige adipose formation. White adipocytes are able to sense physical attributes of 3D environment, including mechanical forces[54]. Adipose tissue ECM in collagen VI knockout mice is characterized by decreased stiffness resulting in enlarged adipocytes without the typically associated necrosis and inflammation[55]. It is also possible that properties other than stiffness that vary with crosslinker concentration could

drive cell behavior, such as resistance to nutrient transport. However, there was little differences in the estimated diffusion coefficients of insulin between the hydrogel conditions. Regardless, these *in vitro* findings support that the properties of the substrate influences adipocyte beiging. This information will be used to further refine our approach for engineering beige adipose tissue.

In addition to the beige adipose markers, the cells expressed adiponectin and PPARG in 3D culture. Adiponectin upregulation and absence of Pref-1 a marker associated with preadipocytes, indicates that the ASCs differentiated into adipocytes. Lipid staining showed both multilocular and unilocular lipid storage in the differentiated cells. Unlike beige adipose markers, expression of these more general adipocyte markers did not vary with hydrogel stiffness. Adiponectin has been suggested to exhibit insulin-sensitizing properties. When combined with the expression of beige adipocyte markers, this suggests the formation of adipose tissue with appropriate metabolic function.

Conclusion

ASCs were differentiated into beige adipocytes in 3D PEGDA hydrogels with mechanical properties approximating the native adipose environment. The cells expressed ECM protein genes and were viable for nearly three weeks in the absence of hydrogel modifications. Beige adipocytes could be generated in the hydrogels and the expression of beige adipocyte markers varied with hydrogel composition. Overall these results are a first step towards engineering beige adipose tissue.

Acknowledgements

This work was funded, in part, by the University of Chicago Diabetes Research and Training Center (NIH, P30 DK020595), the University of Chicago Institute for Translational Medicine (NIH, CTSA UL1 TR000430), The Pritzker Institute of Biomedical Science and Engineering, and the Veterans Administration.

References

1. Cawley J, Meyerhoefer C. J Health Econ. 2012; 31:219–230. [PubMed: 22094013]
2. Gunawardana SC, Piston DW. Am J Physiol Endocrinol Metab, American Journal of Physiology - Endocrinology and Metabolism. 2015:ajpendo 00570 02014.
3. Feige, JN.; Lagouge, M.; Canto, C.; Strehle, A.; Houten, SM.; Milne, JC.; Lambert, PD.; Mataki, C.; Elliott, PJ.; Auwerx, J. Cell Metab. Vol. 8. United States: 2008. p. 347-358.
4. Gunawardana SC. World J Diabetes. 2014; 5:420–430. [PubMed: 25126390]
5. Sacks, H.; Symonds, ME. Diabetes. Vol. 62. United States: 2013. p. 1783-1790.
6. Richard D, Monge-Roffarello B, Chechi K, Labbe SM, Turcotte EE. Front Endocrinol (Lausanne). 2012; 3:36. [PubMed: 22654862]
7. Patrick CW. Seminars in Surgical Oncology. 2000; 19:302–311. [PubMed: 11135487]
8. Toriyama K, Kawaguchi N, Kitoh J, Tajima R, Inou K, Kitagawa Y, Torii S. Tissue Engineering. 2002; 8:157–165. [PubMed: 11886663]
9. Masuda T, Furue M, Matsuda T. Tissue Engineering. 2004; 10:1672–1683. [PubMed: 15684676]
10. Alhadlaq A, Tang M, Mao JJ. Tissue Engineering. 2005:11.
11. Hemmrich K, von Heimburg D, Rendchen R, Di Bartolo C, Milella E, Pallua N. Biomaterials. 2005; 26:7025–7037. [PubMed: 15964623]
12. Brandl FP, Seitz AK, Tessmar JKV, Blunk T, Gopferich AM. Biomaterials. 2010; 31:3957–3966. [PubMed: 20170951]

13. Choi JH, Gimble JM, Lee K, Marra KG, Rubin JP, Yoo JJ, Vunjak-Novakovic G, Kaplan DL. Tissue Engineering Part B-Reviews. 2010:16.
14. Wang XL, Reagan MR, Kaplan DL. Journal of Mammary Gland Biology and Neoplasia. 2010; 15:365–376. [PubMed: 20835885]
15. Sorrell JM, Baber MA, Traktuev DO, March KL, Caplan AI. Biomaterials. 2011; 32:9667–9676. [PubMed: 21959010]
16. Ladewig K, Abberton K, O'Connor AJ. Journal of Biomaterials and Tissue Engineering. 2012; 2:1–13.
17. Wu I, Nahas Z, Kimmerling KA, Rosson GD, Elisseeff JH. Plastic and Reconstructive Surgery. 2012:129.
18. Lilja HE, Morrison WA, Han XL, Palmer J, Taylor C, Tee R, Moller A, Thompson EW, Abberton KM. Stem Cells and Development. 2013; 22:1602–1613. [PubMed: 23231040]
19. Uriel S, Huang JJ, Moya ML, Francis ME, Wang R, Chang SY, Cheng MH, Brey EM. Biomaterials. 2008; 29:3712–3719. [PubMed: 18571717]
20. Seale, P.; Lazar, MA. Diabetes. Vol. 58. United States: 2009. p. 1482-1484.
21. Cesari F. Nature Reviews Molecular Cell Biology. 2008; 9:742–742.
22. Harms M, Seale P. Nat Med. 2013; 19:1252–1263. [PubMed: 24100998]
23. Cypess AM, Lehman S, Williams G, Tal I, Rodman D, Goldfine AB, Kuo FC, Palmer EL, Tseng Y-H, Doria A, Kolodny GM, Kahn CR. New England Journal of Medicine. 2009; 360:1509–1517. [PubMed: 19357406]
24. Himms-Hagen J, Cui J, Danforth E Jr. Taatjes DJ, Lang SS, Waters BL, Claus TH. Am J Physiol. 1994; 266:R1371–1382. [PubMed: 7910436]
25. Seale P, Conroe HM, Estall J, Kajimura S, Frontini A, Ishibashi J, Cohen P, Cinti S, Spiegelman BM. J Clin Invest. 2011; 121:96–105. [PubMed: 21123942]
26. Spiegelman BM. Diabetes. 62:1774–1782. [PubMed: 23704518]
27. Wu J, Cohen P, Spiegelman BM. Genes Dev. 27:234–250. [PubMed: 23388824]
28. Bi P, Shan T, Liu W, Yue F, Yang X, Liang XR, Wang J, Li J, Carlesso N, Liu X, Kuang S. Nat Med. 2014; 20:911–918. [PubMed: 25038826]
29. Wu, J.; Bostrom, P.; Sparks, LM.; Ye, L.; Choi, JH.; Giang, AH.; Khandekar, M.; Virtanen, KA.; Nuutila, P.; Schaart, G.; Huang, K.; Tu, H.; van Marken Lichtenbelt, WD.; Hoeks, J.; Enerback, S.; Schrauwen, P.; Spiegelman, BM. Cell. Vol. 150. 2012 Elsevier Inc; United States: 2012. p. 366-376.
30. Lidell, ME.; Betz, MJ.; Dahlqvist Leinhard, O.; Heglind, M.; Elander, L.; Slawik, M.; Mussack, T.; Nilsson, D.; Romu, T.; Nuutila, P.; Virtanen, KA.; Beuschlein, F.; Persson, A.; Borga, M.; Enerback, S. Nat Med. Vol. 19. United States: 2013. p. 631-634.
31. Keipert S, Jastroch M. Biochim Biophys Acta. 2014; 1837:1075–1082. [PubMed: 24530356]
32. Lee CY, Teymour F, Camastral H, Tirelli N, Hubbell JA, Elbert DL, Papavasiliou G. Macromolecular Reaction Engineering. 2014; 8:314–328.
33. Patel PN, Gobin AS, West JL, Patrick CW. Tissue Engineering. 2005:11.
34. Stosich MS, Bastian B, Marion NW, Clark PA, Reilly G, Mao JJ. Tissue Engineering. 2007; 13:2881–2890. [PubMed: 17824832]
35. Fozdar DY, Wu X, Patrick CW Jr. Chen S. Biomedical Microdevices. 2008; 10:839–849. [PubMed: 18561027]
36. Chiu YC, Cheng MH, Uriel S, Brey EM. J Tissue Viability. 2009
37. Yu G, Wu X, Kilroy G, Halvorsen YD, Gimble JM, Floyd ZE. Methods Mol Biol. 2011; 702:29–36. [PubMed: 21082392]
38. Aune UL, Ruiz L, Kajimura S. J Vis Exp. 2013
39. Ohno, H.; Shinoda, K.; Spiegelman, BM.; Kajimura, S. Cell Metab, A. Vol. 15. 2012 Elsevier Inc; United States: 2012. p. 395-404.
40. Raeber GP, Lutolf MP, Hubbell JA. Acta Biomaterialia. 2007:3.
41. Canal T, Peppas NA. J Biomed Mater Res. 1989; 23:1183–1193. [PubMed: 2808463]

42. Weber LM, Lopez CG, Anseth KS. Journal of Biomedical Materials Research Part A. 2009; 90A: 720–729. [PubMed: 18570315]
43. Livak, KJ.; Schmittgen, TD. Methods. Vol. 25. 2001 Elsevier Science (USA); United States: 2001. p. 402-408.
44. Samani A, Bishop J, Luginbuhl C, Plewes DB. Physics in Medicine and Biology. 2003; 48:2183–2198. [PubMed: 12894978]
45. Alkhouli N, Mansfield J, Green E, Bell J, Knight B, Liversedge N, Tham JC, Welbourn R, Shore AC, Kos K, Winlove CP. American Journal of Physiology-Endocrinology and Metabolism. 2013; 305:E1427–E1435. [PubMed: 24105412]
46. Petrovic, N.; Walden, TB.; Shabalina, IG.; Timmons, JA.; Cannon, B.; Nedergaard, J. J Biol Chem. Vol. 285. United States: 2010. p. 7153-7164.
47. Wilson-Fritch L, Nicoloro S, Chouinard M, Lazar MA, Chui PC, Leszyk J, Straubhaar J, Czech MP, Corvera S. J Clin Invest. 2004; 114:1281–1289. [PubMed: 15520860]
48. Tran TT, Kahn CR. Nat Rev Endocrinol. 2010; 6:195–213. [PubMed: 20195269]
49. Tran TT, Yamamoto Y, Gesta S, Kahn CR. Cell Metab. 2008; 7:410–420. [PubMed: 18460332]
50. Vaicik, MK.; Thyboll Kortesmaa, J.; Moverare-Skrtic, S.; Kortesmaa, J.; Soininen, R.; Bergstrom, G.; Ohlsson, C.; Chong, LY.; Rozell, B.; Emont, M.; Cohen, RN.; Brey, EM.; Tryggvason, K. PLoS One. Vol. 9. United States: 2014. p. e109854
51. Burdick JA, Anseth KS. Biomaterials. 2002; 23:4315–4323. [PubMed: 12219821]
52. Peyton SR, Raub CB, Keschrumrus VP, Putnam AJ. Biomaterials. 2006; 27:4881–4893. [PubMed: 16762407]
53. Salinas CN, Anseth KS. Journal of Tissue Engineering and Regenerative Medicine. 2008; 2:296–304. [PubMed: 18512265]
54. Shoham N, Gefen A. Journal of Biomechanics. 2012:45.
55. Khan T, Muise ES, Iyengar P, Wang ZV, Chandalia M, Abate N, Zhang BB, Bonaldo P, Chua S, Scherer PE. Mol Cell Biol. 2009; 29:1575–1591. [PubMed: 19114551]

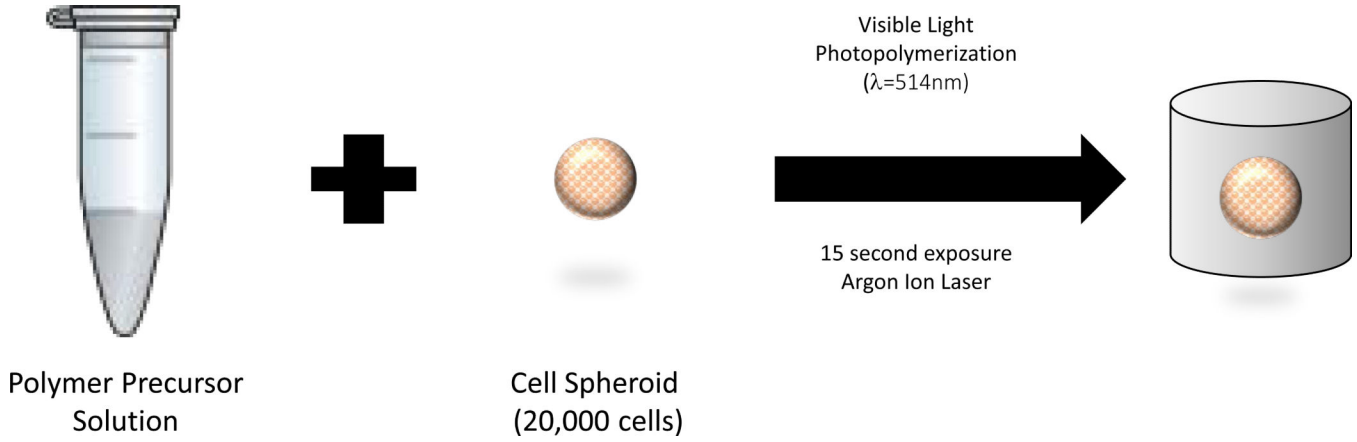

Figure 1.
Cartoon of the procedure for preparing hydrogels containing the cell spheroids.

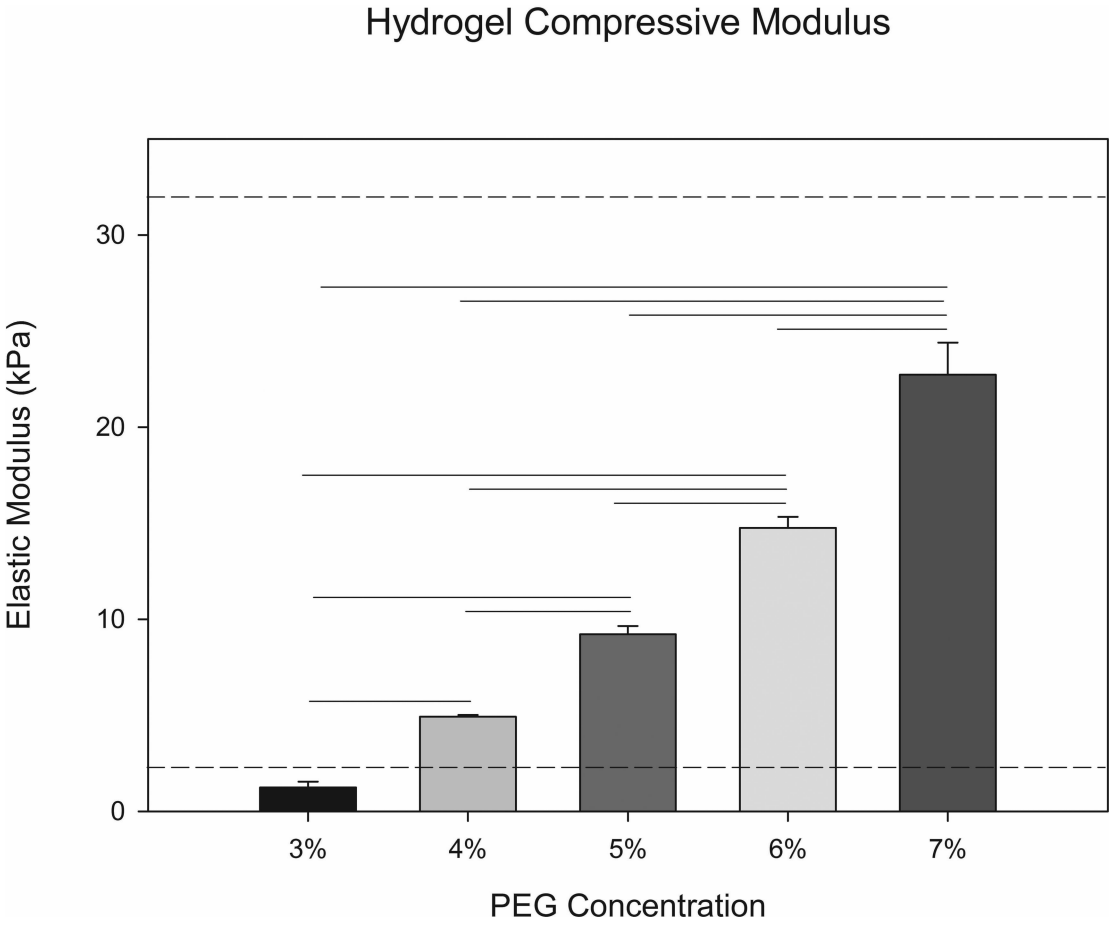

Figure 2.

Compressive modulus of the PEGDA hydrogels as a function of macromer crosslinker concentration. The range of values for adipose tissue are indicated by dotted lines (n=4, $p<0.05$). Standard error shown as error bars.

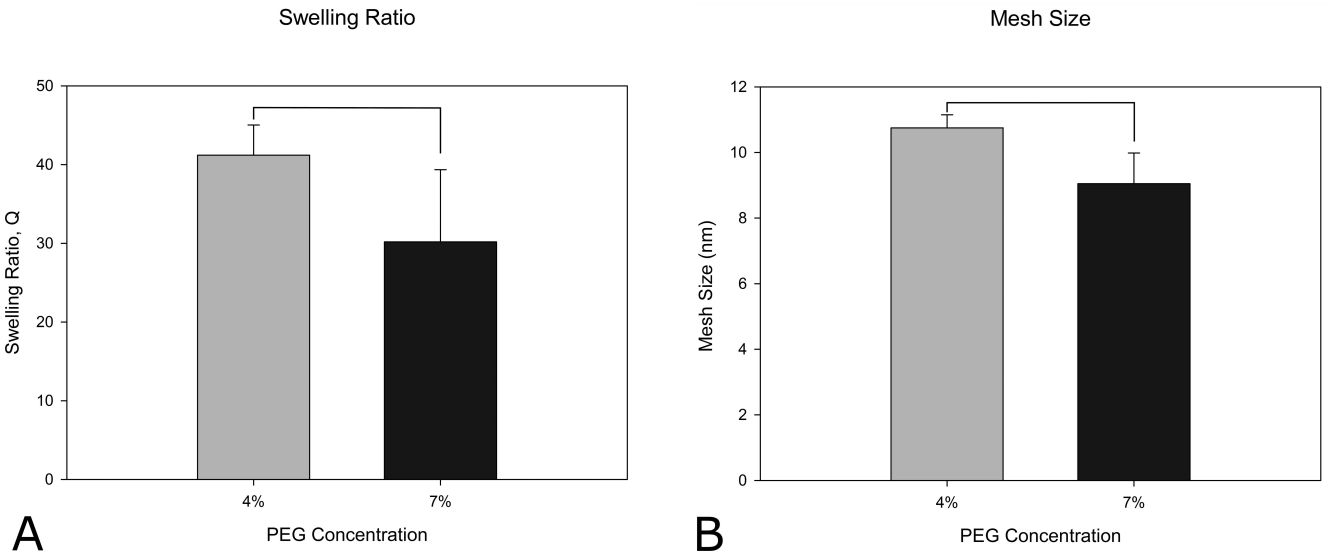

Figure 3.

Swelling ratio (A) and mesh size (B) for 4% and 7% PEGDA macromer concentrations. (n=5, $p<0.05$) Standard deviation shown as error bars. Bars indicate statistically significant differences ($p < 0.05$).

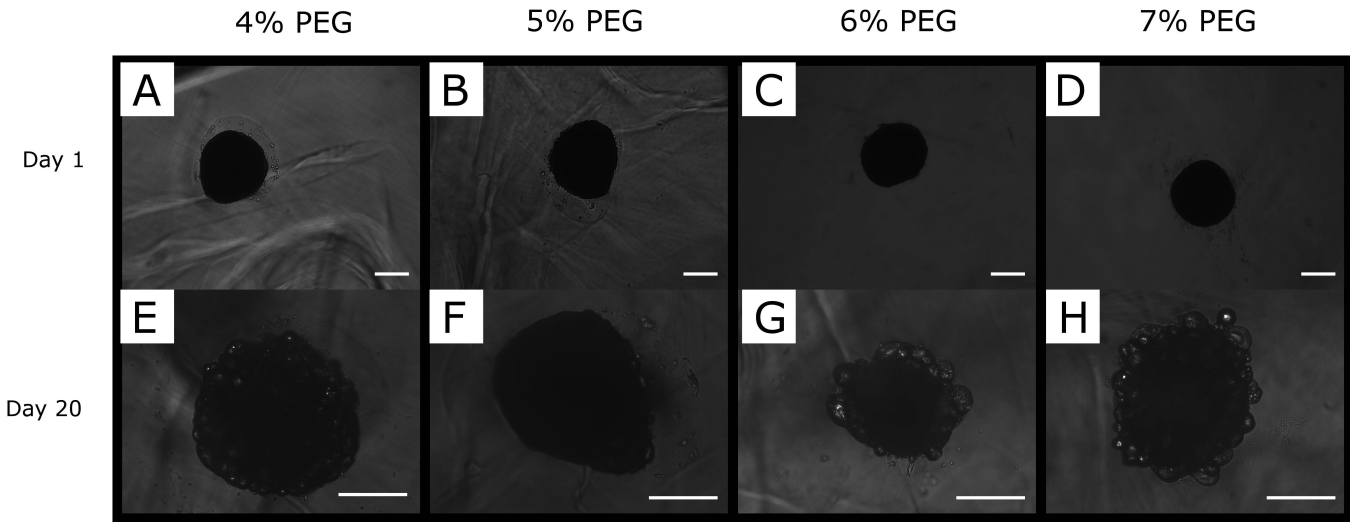

Figure 4.

Brightfield images of cell spheroids day 1 (A,B,C,D) and day 20 (E,F,G,H) in 4%, 5%, 6%, 7% PEGDA hydrogels, respectively. Scale bar is 200 μm.

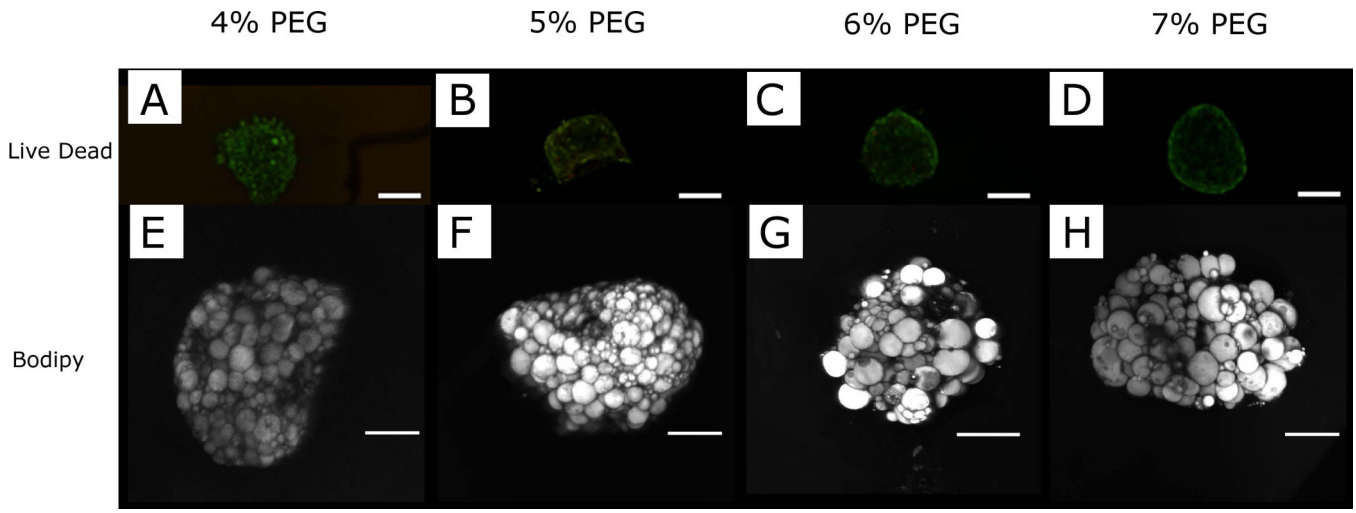

Figure 5.

Viable cells are present throughout the spheroid at day 20 in PEGDA hydrogels as indicated by (A,B,C,D) confocal images of a LIVE/DEAD stain. Live cells stain green and dead cells in red. Scale bar is 200 μm. 98-99% viability was observed in all in all PEGDA concentrations. Bodipy stained spheroids (E,F,G,H) at day 20 in PEGDA hydrogels show the formation of lipid loaded cells with both unilocular and multilocular appearance throughout the spheroid volume. Scale bar is 200 μm.

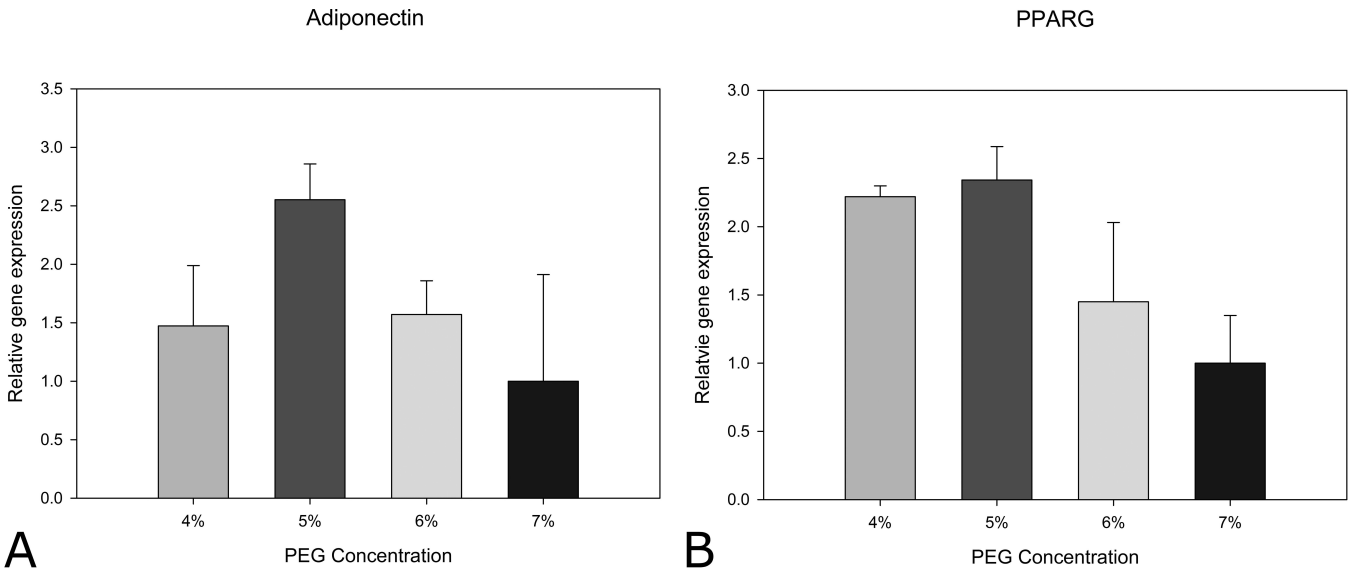

Figure 6.

Adiponectin (A) and PPARG (B) are expressed by in cell spheroids in the PEGDA hydrogels. Data are shown for Day 20 in TZD treated spheroids as a function of PEGDA Concentration. (n=3)

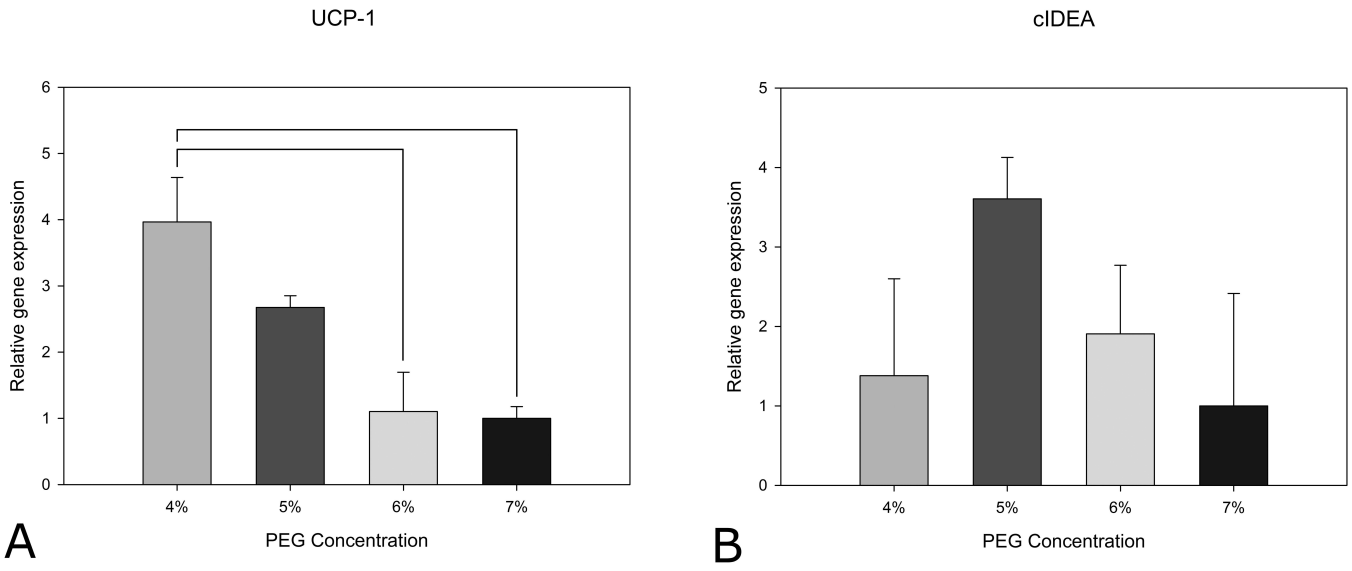

Figure 7.

UCP-1 (A) and cIDEA (B) expression in cell spheroids in the PEGDA hydrogels. Data are shown for day 20 in TZD treated spheroids as a function of PEGDA Concentration. UCP-1 expression decreased with PEGDA concentration. (n=3, statistical significance indicated by lines $p<0.05$)

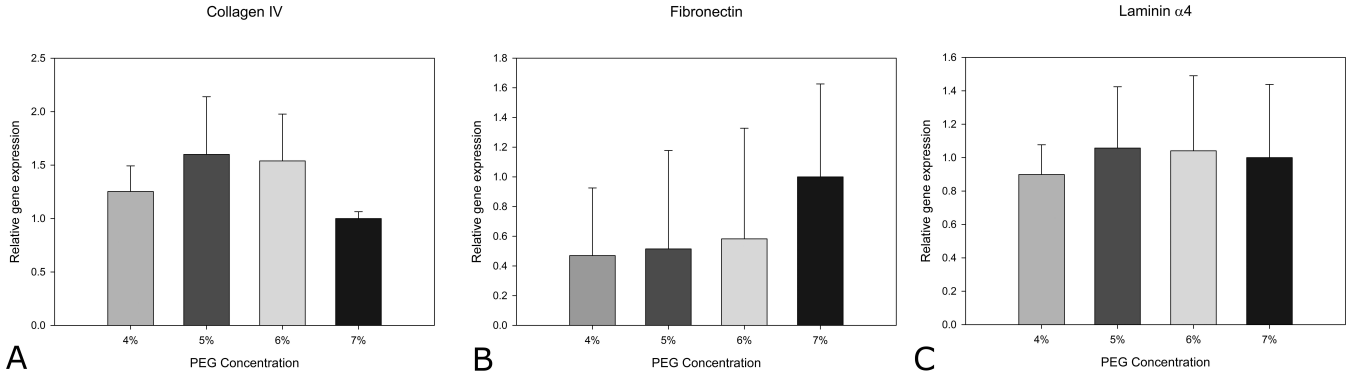

Figure 8.

Collagen iv (A), fibronectin-1 (B), laminin α4 (C) in the PEGDA hydrogels. Data are shown for day 20 in TZD treated spheroids as a function of PEGDA Concentration (n=3).

Table 1

qRT-PCR Primer sequences

gene	Marker Type	Forward Primer	Reverse Primer
18S	reference	AACCCGTTGAACCCCATT	CCATCCAATCGGTAGTAGCG
Adiponectin	adipogenic	GAATCATTATGACGGCAGCA	TCATGTACACCGTGATGTGGTA
PPARG	adipogenic	TCTTCCATCACGGAGAGGTC	GATGCACTGCCTATGAGCAC
Pref-1	preadipocyte	TGTGCAGGAGCATTCGTACT	CGGGAAATTCTGCGAAATAG
Collagen IV	basement membrane	CACATTTTCCACAGCCAGAG	GTCTGGCTTCTGCTGCTCTT
Fibronectin-1	basement membrane	ACTGGATGGGGTGGGAAT	GGAGTGGCACTGTCAACCTC
Lama2	basement membrane	TGCATTCGAAGCAAGATTCA	CTCGAAGGCTCCCAGACT
Lama4	basement membrane	AGGGTGCACATTCTCCTGAC	GAGACTAGCGACTCAGGCGT
cIDEA	beige	TGCTCTTCTGTATCGCCCAGT	GCCGTGTTAAGGAATCTGCTG
PGC1α	beige	TGAGAACCGCTAGCAAGTTT	TGTAGCGACCAATCGGAAAT
PRDM16	beige	ACGCAGAACTTCTCGCTACC	ATGGGAGATGCTGACGGATA
UCP-1	beige	ACTGCCACACCTCCAGTCATT	CTTTGCCTCACTCAGGATTGG